Journal of Rehabilitation in Civil Engineering 13-3 (2025) 69-85

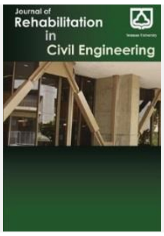

Journal of Rehabilitation in Civil Engineering

Journal homepage: https://civiljournal.semnan.ac.ir/

An Innovative Model to Determine Damping Ratio based on an Experimental Test during Collision

Seyed Mohammad Khatami [1,*]; Hosein Naderpour [2]; Mohammad Reza Zand Moghaddam [3]; Hosein Mousavi Delaziani [4]; Mohsen Maddah [5]

1. Ph.D, University of Applied Science and Technology, Center of Semnan Municipality, Semnan, Iran
2. Professor, Faculty of Civil Engineering, Semnan University, Semnan, Iran
3. Associate Professor, Islamic Azad University, Semnan Branch, Semnan, Iran
4. Ph.D Student, Islamic Azad University, Semnan Branch, Semnan, Iran
5. M.Sc., Semnan Municipality, Semnan, Iran

* Corresponding author: *m61.khatami@gmail.com*

ARTICLE INFO

Article history:
Received: 17 May 2024
Revised: 20 July 2024
Accepted: 07 November 2024

Keywords:
Damping ratio;
Impact force;
Energy dissipation;
Impact velocity;
Experimental test.

ABSTRACT

This study investigates the damping ratio to evaluate impact force and energy absorption during collisions between adjacent buildings under seismic excitation. Experimental tests using different balls and varying heights were conducted to calculate impact velocity. The case of pounding is carried experimentally out and numerically studied based on an experimental test by using different balls and various heights in order to fall and calculate impact velocity. For this challenge, special element is numerically considered which is included to have spring and dashpot. The stiffness of spring and damping ratio of dashpot needs to be accurately calculated for determining impact value and dissipated energy. The cogency of calculation the value of damping ratio is investigated by defining an impact that is basically described and mathematically simulated with a nonlinear viscoelastic model. Using energy role, energy absorption is calculated, and energy dissipation is estimated. Finally, a new equation of motion in field of damping ratio is approximately suggested, and the accuracy of the formula is numerically confirmed and also compared with the results of experimental analyses. For instance, the results of comparison show a 6% error between numerical study and experimental test. In order to investigate the results of evaluation and compare with other equations and experimental test, another study is generally carried out, which describes same peak impact force about 1192 kN in all various results. Finally, different situations by using various parameters are considered to describe the effect of suggested equation.

E-ISSN: 2345-4423

How to cite this article: Khatami, S. M. , Naderpour, H. , Zand Moghdam, M. R. , Mousavi Delaziani, H. and Mddah, M. (2025). An Innovative Model to Determine Damping Ratio based on an Experimental Test during Collision. Journal of Rehabilitation in Civil Engineering, 13(3), 69-85. https://doi.org/10.22075/jrce.2024.34021.2090

1. Introduction

Insufficient separation distance between buildings can lead to significant damage due to collisions during seismic events, a phenomenon known as building pounding. This phenomenon occurs when critical distance cannot cover their relative movements, and large lateral displacement exceeds separation distance between adjacent buildings.

In order to investigate building pounding, many researchers have experimentally tested collision between models with real and unreal scales and also, have numerically presented different equations to calculate impact damping ratio for evaluating pounding, damping and separation distance. Estimation of sufficient gap provides a safety zone between adjacent buildings to avoid a collision during large lateral displacement. In order to calculate impact force during seismic excitation, several equations of motions have been suggested to describe damping ratio and determine the value of energy absorption for showing hysteresis loop of impact and illustrating impact force. Anagnostopolos [1], Maison and Kasai [2], Jankowski [3–5], Jankowski and Mahmoud [6,7], Komodromos et al. [8,9], Ye et al. [10,11], Barros et al. [12], Naderpour et al. [13–17] have experimentally tested some models and also numerically demonstrated building pounding focused on damping ratio in order to suggest an equation of motion to calculate impact force and dissipated energy. In recent years, some other researchers have focused on the effectiveness of external element in order to decline impact force and control pounding hazard [18–27].

According to mentioned studies, there is a significant difference in the zone of impact force and dissipated energy that is caused to justify a new equation to cover all situations and required parameters while representing the most accuracy among suggested formula. As the past studies and equations have been evidently limited to specific parameter as coefficient of restitution, it needs to develop the formula in order to use more parameters such as the body masses, stiffness, velocity and specifically, impact velocity. Developing the equations to find the most accuracy than other equations was a necessary in order to determine impact force and dissipated energy during pounding. In this study, focused on the past equations and based on cyclic process, a new formula is suggested, and the accuracy of the equation is confirmed by using two numerical ways. In here, it can be considered that providing specific situations for adjacent structures, which are built close to each other, is able to control lateral displacement and prevent pounding as critical distance between them, using bumper and provide base isolation system but damping term is used even for mentioned situations and can be used in structural rehabilitation.

2. Existing equation

The majority of researchers have usually described a special element with consisting of a spring and dashpot to investigate a collision between two bodies during seismic excitation in order to simulate impact and calculate energy absorption. When bodies show large lateral displacement, they probably exceed the gap size between them and collision accrues. The general formula to calculate impact force is normally proposed by:

$$F_{imp} = k_s.\delta(t) + c_{imp}.\dot{\delta}(t) \tag{1}$$

where $k_s$and $c_{imp}$are stiffness of spring and damping of dashpot, respectively. In the equation, $\delta(t)$ and $\dot{\delta}(t)$ also explain lateral displacement and velocity, respectively. The power of n has been recommended to be 1.5.

The second term of the formula depends on damping of dashpot, which comes back to damping ratio and is calculated by:

$$c_{imp} = 2.\zeta_{imp}.\sqrt{k_s.M_{eq}} \tag{2}$$

In this equation, $\zeta$is the damping ratio and $M_{eq}$is determined by two body masses, which is $\frac{m_i m_j}{m_i+m_j}$. In order to demonstrate damping ratio, many researchers have numerically presented equation of motions, which are shown by *CR* and is defined by the ratio of impact, before and after the collision. In fact, *CR* shows elastic or inelastic impact as $0 < CR = \frac{\dot{\delta}_{before}}{\dot{\delta}_{after}} < 1$.

According to equation (2), Anagnostopolos [1] has proposed a damping ratio based on a linear viscoelastic model of impact, which was described as:

$$\zeta_{imp} = -\frac{ln(CR)}{\sqrt{\pi^2+(ln(CR))^2}} \tag{3}$$

Based on equation (2), Seyed mahmoud and Jankowski [7] has suggested another equation, called modified linear viscoelastic model, which is expressed by:

$$\begin{cases} F_{imp} = k_s.\delta(t) + c_{imp}.\dot{\delta}(t) \rightarrow \dot{\delta}(t) > 0 \\ \quad F_{imp} = k_s.\delta(t) \rightarrow \dot{\delta}(t) \leq 0 \end{cases} \tag{4}$$

$$\zeta_{imp} = \frac{(1-CR^2)}{CR(CR(\pi-2)+2)} \tag{5}$$

On the other hand, Jankowski [3] has presented a nonlinear viscoelastic model of impact and has numerically shown that the second term of equation (1) is only activated during the approach period. Consequently, the damping ratio is explained as:

$$\begin{cases} F_{imp} = \bar{\beta}.\delta(t)^{1.5} + c_{imp}.\dot{\delta}(t) \rightarrow \dot{\delta}(t) > 0 \\ \quad F_{imp} = \bar{\beta}.\delta(t)^{1.5} \rightarrow \dot{\delta}(t) \leq 0 \end{cases} \tag{6}$$

$$\zeta_{imp} = \frac{9\sqrt{5}}{2}.\frac{(1-CR^2)}{CR(CR(9\pi-16)+16)} \tag{7}$$

Barros et al. [12] has also suggested a new equation based on the nonlinear viscoelastic model and justified damping ratio using the coefficient of restitution which is written as:

$$\zeta_{imp} = (\frac{(1-CR^2)}{CR(\sqrt{\pi}(\frac{CR}{2}+\frac{1}{\pi})-CR)})^2 \tag{8}$$

Based on equations (3), (5), (7) and (8), hysteresis model of impact is depicted in order to compare among models as it can be seen in Fig. [1].

Different equations have shown various results with the same CR. It seems that it is a need to justify an equation of motion based on CR, which can cover all the responses accurately.

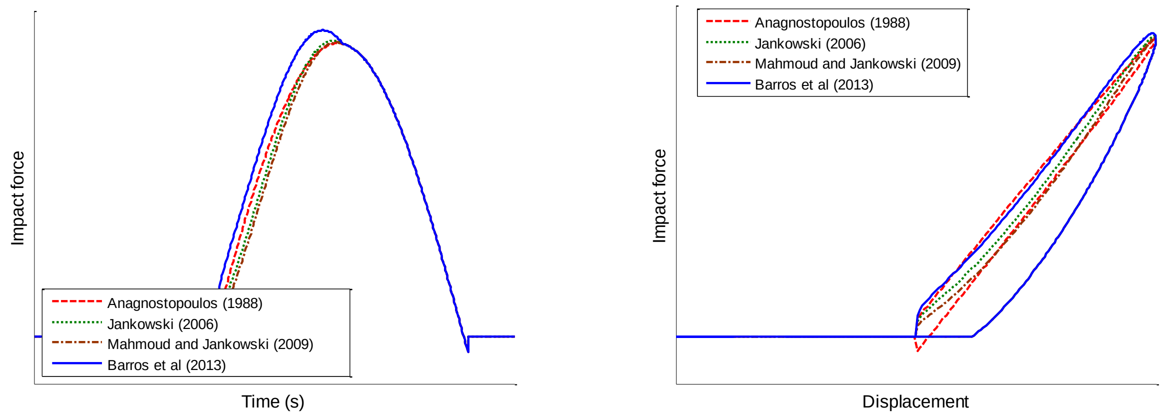

Fig. 1. Comparison of hysteresis loops of used equations (3), (5), (6) and (7).

3. Proposed damping ratio formula

To investigate the accuracy of various formulas, experimental tests were conducted using two balls made of different materials. Concrete and plastic balls, each with the same mass, were dropped from heights of 50, 150, and 250 cm onto a rigid surface. For this challenge, the value of dissipated energy of the numerical analysis are mathematically calculated and compared with the value of dissipated energy of impact experimental conducted by dropping balls. The materials of balls are considered to be concrete and plastic with same masses onto a rigid surface. Balls were dropped from 50, 150 and 250 cm and their impact velocities are numerically determined.

For the purpose of calculation of dissipated energy, a completed cycle of dropping ball is assumed to divide into three parts.

The main physics equation of dropping ball is defined as the follow:

$$mgh_i + \frac{1}{2}mv_i^2 = mgh_j + \frac{1}{2}mv_j^2 \tag{9}$$

So, there is:

$$\begin{cases} gh_i = \frac{1}{2}v_i^2 \rightarrow First - part \\ \frac{1}{2}v_i^2 - \Delta E = \frac{1}{2}v_j^2 \rightarrow Second - part \\ \frac{1}{2}v_j^2 = gh_j \rightarrow Third - part \end{cases} \tag{10}$$

In here, velocities are calculated by:

$$v_i = \sqrt{2gh_i} \tag{11}$$

And finally, dissipated energy is determined based on:

$$\Delta E = \frac{1}{2}(v_i^2 - v_j^2) \tag{12}$$

On the other hand, it is assumed that the enclosed area of loop is energy absorption of each collision which should be equal with kinetic energy loss when two bodies collide with each other and is written by the following form:

$$E = \frac{1}{2}.M_{eq}.(1 - CR^2).\dot{\delta}_{imp}^2 \tag{13}$$

$M_{eq}$is determined by two body masses, which is $\frac{m_i m_j}{m_i+m_j}$. The schematic form of energy absorption is obviously seen in Fig. [2].

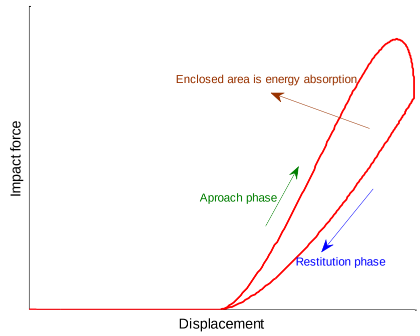

Fig. 2. Schematic form of energy absorption.

If energy absorption and dissipated energy become to equal, the equation used in zone of damping ratio can be selected as the most accurate formula.

For this challenge, balls are selected to have same masses and dropped from various height in order to calculate velocities as it is described in Table [1] and the schematic shape of test is seen in Fig. [3].

Table 1. The results of experimental test.

$m(g)$	$H_1(cm)$	$H_2(cm)$	$v_1(cm/s)$	$v_2(cm/s)$	CR	E
	50	48.9	31.32	40.68	0.9889	2266.11
210	150	111.3	54.24	46.73	0.8613	79725.8
	250	167.4	70.03	57.3	0.8182	170164.3

In here, two different phases are mathematically generated based on velocity. Approach phase is accorded when velocity is positive and restitution phase is also shown when velocity is negative. Enclosed area is calculated during approach and restitution phase which is shown by:

$$A = \int_0^{\delta_m} k_s.\delta^{1.5}\,d\delta - \int_0^{\delta_m}(k_s.\delta^{1.5} + \zeta_{imp}.\delta^{1.5}.\dot{\delta})d\delta = -\int_0^{\delta_m} \zeta_{imp}.\delta^{1.5}.\dot{\delta}d\delta \tag{14}$$

So, as it was noted, kinetic energy is compared with energy absorption which is expression by:

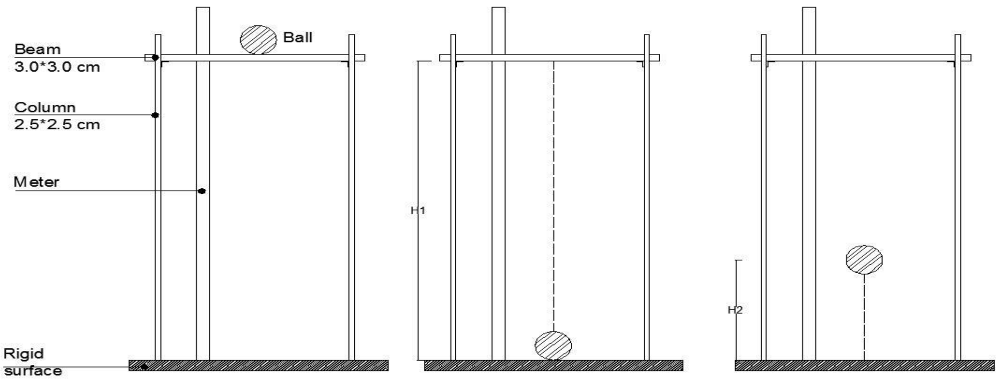

Fig. 3. Schematic set up of experimental test.

$$\frac{1}{2}.M_{eq}.(1-CR^2).\dot{\delta}_{imp}^2 = -\int_0^{\delta_m} \zeta_{imp}.\delta^{1.5}\dot{\delta}d\delta \quad (15)$$

On the other hand, when maximum value of the displacement is shown, kinetic energy can be calculated as a plastic impact which is written as the below:

$$\frac{1}{2}.M_{eq}.\dot{\delta}_{imp}^2 = \int_0^{\delta_m} k_s.\delta^{1.5}.d\delta \quad (16)$$

In here, equation (12) is generally solved and maximum displacement is created by:

$$\delta_m = \left(1.25.\frac{M_{eq}\dot{\delta}_{imp}^2}{k_s}\right)^{0.4} \quad (17)$$

Finally, in approach phase, it is considered that velocity is positive, so we have:

$$\int_0^{\delta_m} k_s.\delta^{1.5}d\delta + \frac{1}{2}.M_{eq}.\dot{\delta}_{approach}^2 = \frac{1}{2}.M_{eq}.\dot{\delta}_{imp}^2 \rightarrow \dot{\delta} > 0 \quad (18)$$

By solving equation (18), velocity is created as:

$$\dot{\delta}_{approach} = \sqrt{\dot{\delta}_{imp}^2 - \frac{0.8.k_s.\delta^{2.5}}{M_{eq}}} \quad (19)$$

After impact, velocity is moved to negative as restitution phases and declined by using a decrement factor as the below form:

$$\dot{\delta}_{restitution} = -\frac{1}{\mu.CR^{\alpha}}.\dot{\delta}_{approach} \rightarrow -\frac{1}{\mu.CR^{\alpha}}.\sqrt{\dot{\delta}_{imp}^2 - \frac{0.8.k_s.\delta^{2.5}}{M_{eq}}} \quad (20)$$

In the equation (20), two parameters are assumed to be $0.065 < \mu < 0.075$ and $2.5 < \alpha < 3$. So, equation (17) is changed to be:

$$\frac{1}{2}.M_{eq}.(1-CR^2).\dot{\delta}_{imp}^2 = \int_0^{\delta_m} \frac{\zeta_{imp}.\delta^{1.5}}{0.071.CR^{2.68}}.\sqrt{\dot{\delta}_{imp}^2 - \frac{0.8.k_s.\delta^{2.5}}{M_{eq}}}d\delta \quad (21)$$

By using equation (17), impact velocity will be:

$$\dot{\delta}_{imp}^2 = \frac{0.8.\delta_m^{2.5}.k_s}{M_{eq}} \quad (22)$$

Then, equation (22) into equation (21) will be:

$$\frac{1}{2}.M_{eq}.(1-CR^2).\dot{\delta}_{imp}^2 = 14.084\int_0^{\delta_m} \frac{\zeta_{imp}.\delta^{1.5}}{CR^{2.68}}.\sqrt{\frac{0.8.\delta_m^{2.5}.k_s}{M_{eq}} - \frac{0.8.k_s.\delta^{2.5}}{M_{eq}}}d\delta \quad (23)$$

Which becomes:

$$\frac{1}{2}.M_{eq}.(1-CR^2).\dot{\delta}_{imp}^2 = 14.084.\frac{\zeta_{imp}}{CR^{2.68}}.\sqrt{\frac{0.8.k_s}{M_{eq}}}\int_0^{\delta_m} \delta^{1.5}\sqrt{(\delta_m^{2.5} - \delta^{2.5})}\,d\delta \quad (24)$$

In this equation, the integral term of formula is solved and finally, the equation is formed as follows:

$$\frac{1}{2}.M_{eq}.(1-CR^2).\dot{\delta}_{imp}^2 = 3.7563.\frac{\zeta_{imp}}{CR^{2.68}}.\sqrt{\frac{0.8..k_s}{M_{eq}}}.\left(\frac{1.25.M_{eq}.\dot{\delta}_{imp}^2}{k_s}\right)^{1.5} \quad (25)$$

And now, simplified equation is created as:

$$\frac{1}{2}.(1-CR^2)=4.6954.\frac{\zeta_{imp}}{CR^{2.68}}.\frac{\dot{\delta}_{imp}}{k_s} \tag{26}$$

Finally, damping ratio is obviously created by:

$$\zeta_{imp}=0.1065\frac{k_s.(1-CR^2)}{\dot{\delta}_{imp}}.CR^{2.68} \tag{27}$$

On the other hand, in order to investigate the accuracy of formula, following an iterative procedure and basing on stiffness of spring and impact velocity, another process is mathematically carried out to confirm the equation by the formula:

$$\zeta_{imp}^{'}=\bar{\omega}.\frac{k_s(1-CR)}{\dot{\delta}_{imp}} \tag{28}$$

Specifically for finding the value of ϖ, the process is started and equations are solved to reach a new equation of motion which is explained by the below form:

$$\varpi=0.14.CR^{2.907} \tag{29}$$

Therefore, generally form of equation will be as:

$$\zeta_{imp}^{'}=0.14.\frac{k_s.(1-CR)}{\dot{\delta}_{imp}}.CR^{2.907} \tag{30}$$

So, impact force will be::

$$\begin{cases} F_{imp}=k_s.\delta^{1.5}(t)+c_{imp}.\dot{\delta}(t)\rightarrow\delta>0-\dot{\delta}<0 \\ F_{imp}=k_s.\delta^{1.5}(t)\rightarrow\delta>0-\dot{\delta}>0 \\ F_{imp}=0\rightarrow\delta<0 \end{cases} \tag{31}$$

4. Verification

In here, by focusing on equation (24) and in order to investigate the accuracy of formula, two different ways are carried numerically out based on energy dissipation and peak impact forces. For this challenge, CRVK program is basically used and developed to perform dynamic analyses and solve impact simulation.

Firstly, in order to determine the impact force and energy dissipation, an impact between two bodies is simulated and the hysteresis loop is depicted. It is assumed that the dissipated energy is approximately expressed by the enclosed area of the hysteresis curve due to the impact. On the other hand, the kinetic energy loss due to the impact was demonstrated by Goldsmith [19], which was seen as:

$$E=\frac{1}{2}.M_{eq}.(1-CR^2).\dot{\delta}_{imp}^2 \tag{32}$$

It is obviously confirmed that the dissipated energy during the impact has to be equal to the kinetic energy calculated by equation (25). Undoubtedly, if both energies become equal to each other, it shows the accuracy of the impact damping ratio. Based on Naderpour et al. [17]; stiffness of spring is calculated by using equal masses, which is described as:

$$k_s=88.782.M_{eq}^{0.924} \tag{33}$$

Let us assume two bodies with 170 and 320 kg. An equal mass is calculated to be 111 kg, and subsequently, the stiffness of spring will be 6922 kN/mm1.5. In order to calculate energy by equation (25), CRVK program is used and by having equal mass, impact velocity is numerically determined. The program needs to have the value of velocity before impact and selected CR as inputs, and after starting the simulation of process; the equation of the value of impact velocity is analyzed and solved. Finally, the result is also plotted with a special curve as the below (Fig. [4].).

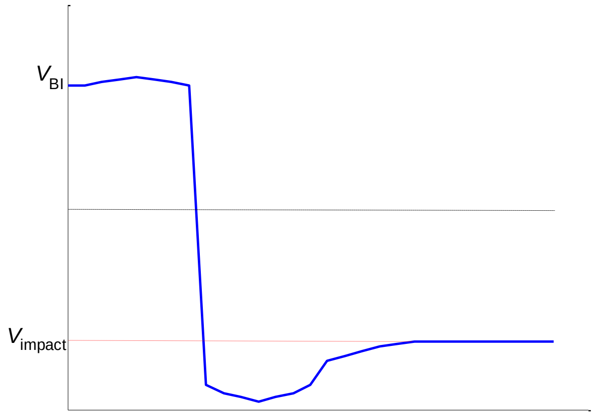

Fig. 4. Impact velocity based on the value of velocity before impact and CR.

Now, by using *CRVK* program, an impact is simulated, and the damping ratio is mathematically determined. Consequently, the damping value is calculated and the impact formula is numerically solved. For example, CR is assumed to be 0.4 and impact force is 1 m/s. now we have:

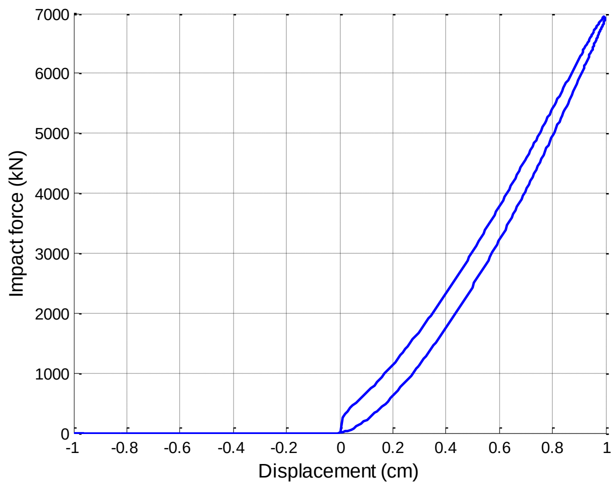

Fig. 5. Hysteresis loop of impact based on impact force- displacement.

In this case, the enclosed area (A) is 47.63, and kinetic energy (E) is calculated to be 46.62. As it was noted, selected CR is 0.4, and the calculated CR is 0.3764, which shows an error about 6% (Fig. [5]).

The accuracy of the equation is observed by the Fig. [6]. Selected CR and calculated CR are compared with each other, which show an acceptable response. In fact, CRVK solves the equation based on an impact, which was simulated by specific CR and a cyclic program is used to calculate another CR, which are compared with each other to show the accuracy of formula.

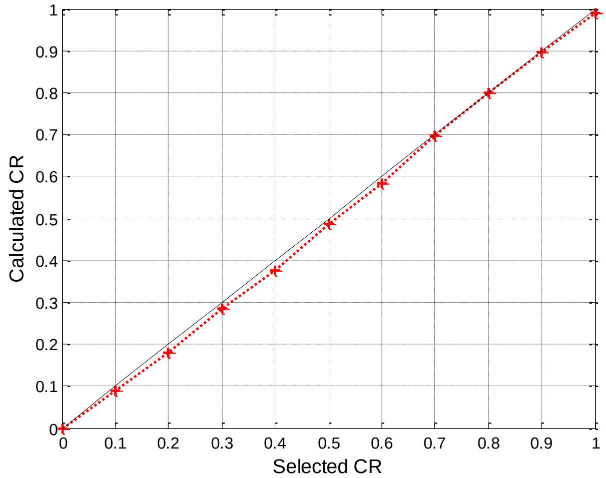

Fig. 6. Accuracy of the proposed damping ratio by numerical analysis based on dissipated energy.

Secondly, peak impact forces of the simulation are calculated and listed based on the coefficient of restitution. Different CR can justify different responses in terms of impact and dissipated energy. In fact, an equation can be accepted that the results of analyses show the same responses by using different CR. In the following, an impact is performed again by CRVK and peak impact forces are numerically calculated. All the results are collected and depicted in the figure.

The results of analyses are compared with each other and shown the maximum impact forces have accrued in all equations by using the least value of the coefficient of restitution. As it is seen, different equations have obviously shown various peak impact forces. For example, by using CR=0.4, peak impact force has been calculated as 17056, 8513, 7749 and 6927 kN for equation (5), (8), (9) and (14), respectively. It is mentioned that different CR have explained different peak impact forces in equations (5), (8) and (9), by a decreasing pattern from 0.1 to 0.9, but equation (14) has represented a line, which can prove the accuracy of formula and confirm proposed formula (Fig. [7]). In other words, selecting coefficient of restitution of 0 to 0.3 makes a differences in peak impact force and more than 0.3, the results are normally calculated.

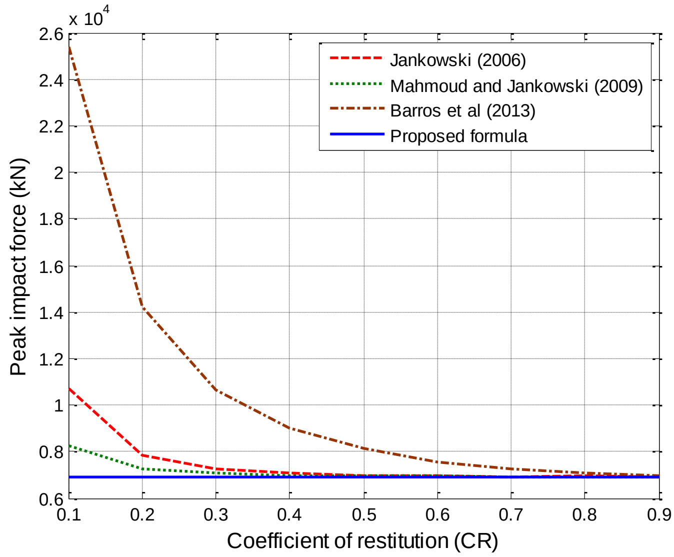

Fig. 7. Accuracy of the proposed damping ratio by numerical analysis based on peak impact force.

The figure shows that the formulations by Barros et al., and Mahmoud and Jankowski result in different peak impact forces for varying coefficients of restitution. On the other hand, the application of the proposed formula has allowed selecting various CR with the same response. Consequently, it must be underlined that the proposed formula can be accepted in all of cases and coefficient of restitutions.

5. Impact test

In this part, the experimental test is theoretically investigated which was similar with Jankowski test [20] and has been explained in previously part. The test was carried out with same shape and different mass, height and velocity (Fig. [8]).

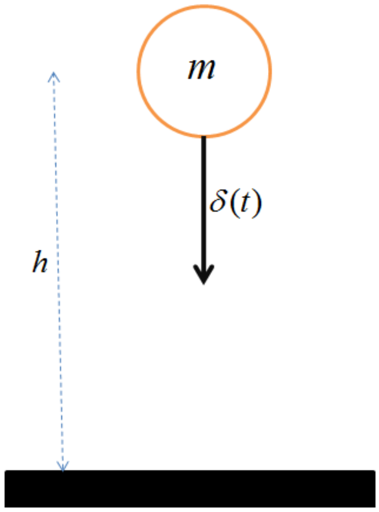

Fig. 8. Model of a ball falling onto a rigid surface.

In order to evaluate impact, the model of a ball falling onto a rigid surface, calibrated by experimental test, is mathematically considered which becomes:

$$m\ddot{\delta}(t) + F_{imp} = mg \tag{34}$$

In this equation, m is the ball mass, Fimp denotes impact force, g and $\ddot{\delta}(t)$ are an acceleration of gravity and vertical acceleration, respectively. The difference among various used models is evaluated by determining the normalized root mean square (RMS) error [21] which is shown by:

$$RMS = \frac{\sqrt{\sum_{i=1}^{NV}(H_i - \bar{H}_i)^2}}{\sqrt{\sum_{i=1}^{NV} H_i^2}}.100\% \tag{35}$$

Where H_i and $\bar{H}_i$ denote the value from the time history record obtained from the experiment and from the numerical analysis, respectively. NV is also a number of values in these history records.

In order to evaluate the results of impacts and comparison among equations and experimental analyses, the properties of experimental are used (Ball of mass is 210 g and the velocity is 46.73 cm/s.) as input for equations and an impact is numerically simulated. The stiffness of spring and impact damping ratio based on CR=0.58 is calculated to be $k_s = 4.82 \times 10^8 N/m$ and $\zeta = 0.17$, for linear viscoelastic model (equation (3)), $k_s = 5.03 \times 10^8 N/m$ and $\zeta = 0.43$, for modified linear viscoelastic model (equation (5)), $\bar{\beta} = 6.6 \times 10^{10} N/m^{1.5}$ and $\zeta = 0.49$, and $6.6 \times 10^8 N/m^{1.5}$ and $\zeta = 0.2.29$, for nonlinear viscoelastic model of equations (8) and (9), respectively (Fig. [9]).

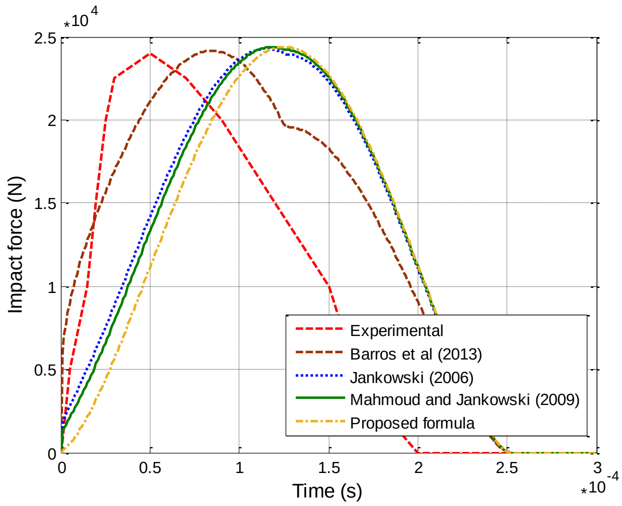

Fig. 9. Pounding force time histories for impact-time among equations and experimental test y steel elements.

The results of impact based on time for all equations in comparison with experimental steel element are shown. In order to calculate the RMS errors, equation (23) is used which shows a 72.2%, 70.4%, 68.1% and 49.8% RMS error for proposed formula, Jankowski, Mahmoud and Jankowski, Barros et al, respectively.

In order to carry out the second comparison between numerical results of models and the experimental result for concrete ball, a new simulation is described and a concrete ball of mass 1.763 kg with 0.13 m/s velocity is defined. The stiffness of spring and impact damping ratio based on CR=0.76 is calculated to be $k_s = 4.91 \times 10^7 N/m$ and $\zeta = 0.09$, for linear viscoelastic model (equation (3)), $k_s = 5.47 \times 10^7 N/m$ and $\zeta = 0.19$, for modified linear viscoelastic model (equation (5)), $\bar{\beta} = 5.92 \times 10^9 N/m^{1.5}$, and $6.39 \times 10^9 N/m^{1.5}$, for nonlinear viscoelastic model of equations (8) and (9), respectively. The results of impact based on time for all equations in comparison with experimental are shown in Fig. [10].

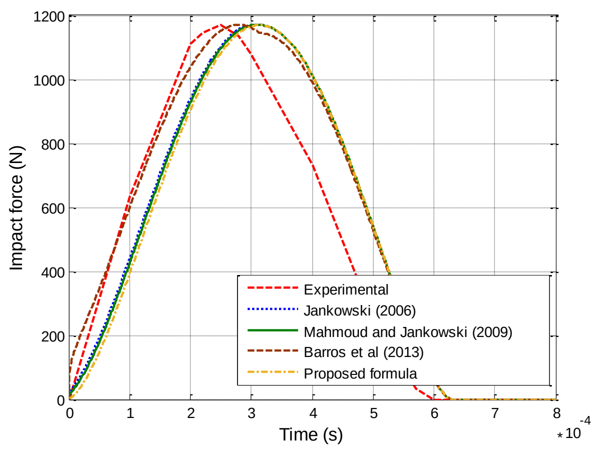

Fig. 10. Pounding force time histories for impact-time among equations and experimental test by concrete elements.

The results of impact based on time for all equations in comparison with experimental concrete element are shown. In order to calculate the RMS errors, equation (23) is used which shows a 36.2%, 36.4%, 35% and 34.5% RMS error for proposed formula, Jankowski, Mahmoud and Jankowski, Barros et al, respectively.

Finally, the results of a timber ball of 0.109 kg with a 0.39 m/s impact velocity is used to be compared with the results of different models. The stiffness of spring and impact damping ratio based on CR=0.61 is calculated to be $k_s = 2.28 \times 10^6 N/m$ and $\zeta = 0.16$, for linear viscoelastic model (equation (3)), $k_s = 2.62 \times 10^6 N/m$ and $\zeta = 0.38$, for modified linear viscoelastic model (equation (5)), $\bar{\beta} = 1.66 \times 10^8 N/m^{1.5}$, and $3.11 \times 10^8 N/m^{1.5}$, for nonlinear viscoelastic model of equations (8) and (9), respectively. The results of impact based on time for all equations in comparison with experimental are shown in Fig. [11].

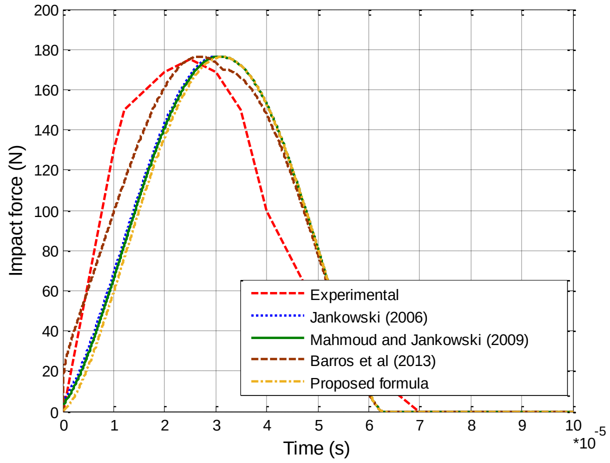

Fig. 11. Pounding force time histories for impact-time among equations and experimental test by timber elements.

The results of impact based on time for all equations in comparison with experimental timber element are shown. In order to calculate the RMS errors, equation (18) is used which shows a 22.1%, 22.3%, 22.4% and 22.7% RMS error for proposed formula, Jankowski, Mahmoud and Jankowski, Barros et al, respectively.

In order to compare the results of displacement and velocity for all models, Kobe earthquake record is used with considering a stiffness of spring and impact damping ratio based on CR=0.65 which is assumed to be $k_s = 1.12 \times 10^8 N/m$, for linear viscoelastic model (equation (3)), $k_s = 1.24 \times 10^8 N/m$, for modified linear viscoelastic model (equation (5)), and $\bar{\beta} = 2.75 \times 10^{10} N^{1.5}/m$, for nonlinear viscoelastic model of equations (8) and (9), respectively (Fig. [12]).

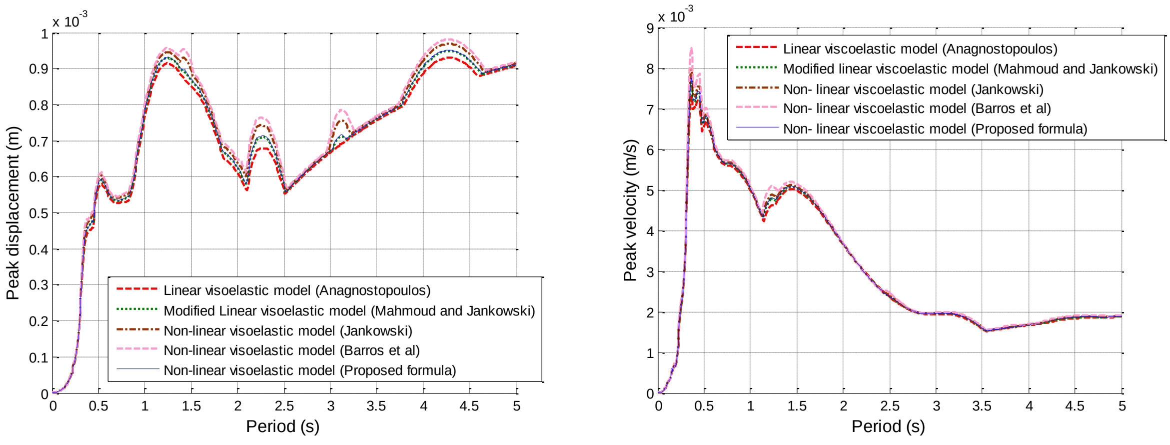

Fig. 12. Peak lateral displacement and velocity with respect to the structural period under different earthquakes.

The peak lateral displacements and velocities were calculated for different periods of colliding structures using mentioned earthquake record. The results of the analyses are presented in Figure (12). The analyzed models show an increasing trend by a growing period in the zone of displacement. On the contrary, velocity shows a suddenly increase from 0 to 0.5 s and a sharp decline to 5 s.

6. Parametric study

In here, the extensive numerical analysis has been conducted by two SDOF dynamic buildings with 1250 and 3150 kg lumped masses that have been separated by a 1 cm gap size. A special link element is assumed to be located at the top level, included by a spring and dashpot. Five earthquake records of the Kobe earthquake of 1995, Elcentro earthquake of 1940, Loma Prieta earthquake of 1989, Parkfield earthquake of 1966 and Sanfernando earthquake of 1971, are used in this paper.

6.1. Effect of lumped mass

According to equations (7), the damping ratio depends directly on the lumped masses during collisions. It can be predicted that changing the value of masses, periods are naturally varied and subsequently, models show different lateral displacement. For instance, a calm increase in the zone of impact force is normally indicated with the growth of the equal mass. In order to get the responses of impacts and compare the results of peak impact forces, different values of the equal masses are considered from the interval 0 to 3000 kg, and the results of forces are listed to be compared among five different earthquake records.

As it is obviously seen, peak impact forces are 19.94, 19.42, 7.78, 6.25 and 3.6 N by using an equal mass of about 3000 kg for Lomaprieta, Parkfield, Elcentro, Sanfernando and Kobe, respectively (Fig. [13]).

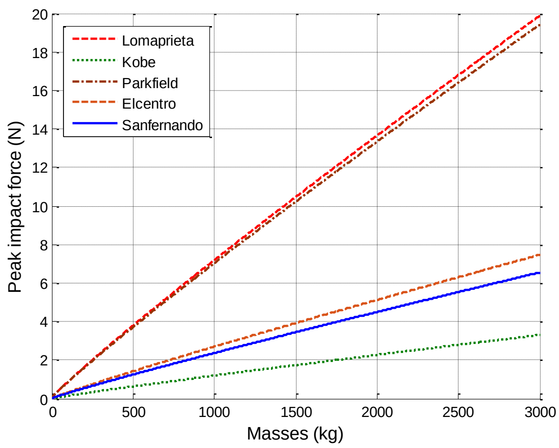

Fig. 13. Peak impact force with increasing lumped masses.

6.2. Effect of coefficient of restitution

As the coefficient of restitution is one of the most important parameters to investigate impact force and has a great effect on the calculation of the impact damping ratio, different values of CR are considered to compare the impact forces during used records. Figure (14) shows that the peak impact forces shows a sharp decrease among CR=0 to 0.3 and after that, slowly grow when the coefficient of restitution is increased. In fact, there is considerable discrepancy in zone of impact force between two different zones, 0 to 0.3 and 0.3 to 1. A similar trend of impact force responses about 47, 46, 23, 18 and 7.5 N are observed for CR=0 to 9.7, 9.65, 3.95, 3.85 and 25 N for CR=0.3 in Lomaprieta, Parkfield, Sanfernando, Elcentro and Kobe, respectively. In continue, a linear response is observed in all records from CR=0.3 to 1, which are 9.7, 9.65, 3.95, 3.85 and 25 N for Lomaprieta, Parkfield, Sanfernando, Elcentro and Kobe, respectively (Fig. [14]).

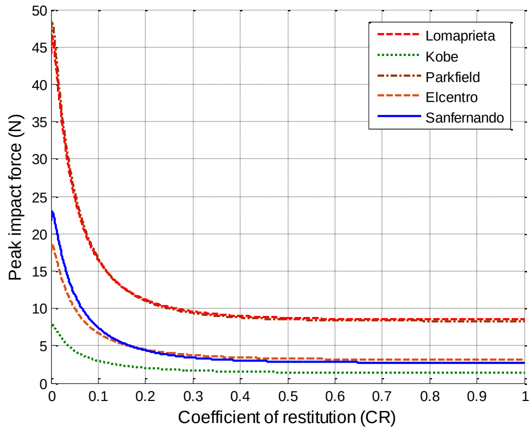

Fig. 14. Peak impact force with an increasing coefficient of restitution.

6.3. Effect of period

In order to evaluate the effectiveness of the period, this parameter is varied from 0 to 1 s. Peak impact forces have shown a light increase in the zone of 0 to 0.7 s, between 0 to 1.5 N, and suddenly, curves have sharply grown from 1.5 to 8.75, 8.65, 3.2, 2.9 and 1.7 in Lomaprieta, Parkfield, Elcentro, Sanfernando and Kobe, respectively (Fig. [15]).

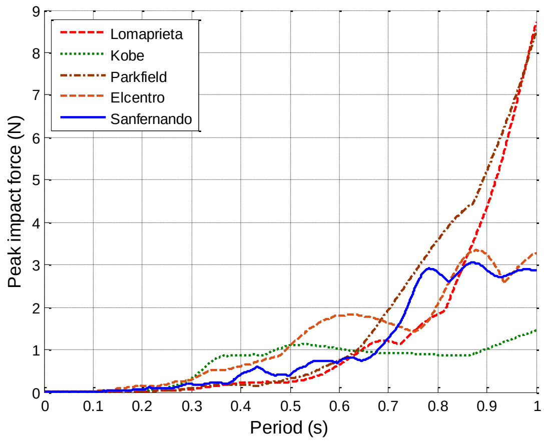

Fig. 15. Peak impact force with increasing period of model.

7. Conclusion

This study numerically and experimentally investigated the validity of a new equation of motion for determining the damping ratio in building pounding scenarios, focusing on impact force and energy absorption. Based on an experimental test and using a mathematic program, a new equation of motion is suggested, and the accuracy of the formula is confirmed. The accuracy of the equation is numerically investigated by selecting different *CR* and determines energy dissipation, then calculates equal *CR* based on energy role. Special attention of equation is focused significantly on the same response by using the different coefficient of restitutions. The study has shown a considerable discrepancy in terms of impact force with different mass and periods, which can be defined them as two important parameters to calculate impact force with different records while the coefficient of restitution has not provided significant deference. The models present an increasing trend by a growing period in the field of displacement. On the other hand, velocity shows a suddenly increase from 0 to 0.5 s and a sharp decline to 5 s when period is repetitively increased. As suggested equation depends on the coefficient of restitution, the same response by using different CR show the accuracy of the created formula. Investigation of the effectiveness of periods indicates by increasing the mentioned parameter; there is a growing trend in peak impact force, displacement, and velocity. It seems this subject can be continued by considering critical distance between structures to avoid pounding or define a new damping value for rubber bumpers, attached at the contact zone of buildings.

Funding

There was no financial support from the company, university or scientific center.

Conflicts of interest

The author is an Editorial Board Member/Editor-in-Chief/Associate Editor/Guest Editor for Journal of Rehabilitation in Civil Engineering and was not involved in the editorial review or the decision to publish this article.

One of the authors of the article (H. Naderpour) is the " Manager and Editorial Board Member" of the journal. Based on the journal policy, this author was completely excluded from any review process of this article and the review process of this article.

Authors contribution statement

Seyed M. Khatami: Conceptualization, Data curation, Formal analysis, Investigation, Methodology, Project administration, Resources, Software, Supervision, Validation; Visualization; Roles/Writing – original draft, Writing – review & editing.

Hosein Naderpour: Conceptualization, Data curation, Formal analysis, Investigation, Methodology, Project administration, Resources, Software, Supervision, Validation; Visualization; Roles/Writing – original draft, Writing – review & editing.

Mohammad Reza Zand Moghaddam: Resources, Roles/Writing.

Hosein Mousavi Delaziani: Writing – review & editing.

Mohsen Maddah: Writing – review & editing.

References

[1] Anagnostopoulos SA. Pounding of buildings in series during earthquakes. Earthq Eng Struct Dyn 1988;16:443–56. https://doi.org/10.1002/eqe.4290160311.

[2] Kasai K, Maison BF. Building pounding damage during the 1989 Loma Prieta earthquake. Eng Struct 1997;19:195–207. https://doi.org/10.1016/S0141-0296(96)00082-X.

[3] Jankowski R. Non-linear viscoelastic modelling of earthquake-induced structural pounding. Earthq Eng Struct Dyn 2005;34:595–611. https://doi.org/10.1002/eqe.434.

[4] Jankowski R. Pounding force response spectrum under earthquake excitation. Eng Struct 2006;28:1149–61. https://doi.org/10.1016/j.engstruct.2005.12.005.

[5] Jankowski R. Non-linear FEM analysis of earthquake-induced pounding between the main building and the stairway tower of the Olive View Hospital. Eng Struct 2009;31:1851–64. https://doi.org/10.1016/j.engstruct.2009.03.024.

[6] Mahmoud S, Jankowski R. Modified linear viscoelastic model of earthquake-induced structural pounding 2011.

[7] Jankowski R. Experimental study on earthquake-induced pounding between structural elements made of different building materials. Earthq Eng Struct Dyn 2010;39:343–54. https://doi.org/10.1002/eqe.941.

[8] Komodromos P, Polycarpou PC, Papaloizou L, Phocas MC. Response of seismically isolated buildings considering poundings. Earthq Eng Struct Dyn 2007;36:1605–22. https://doi.org/10.1002/eqe.692.

[9] Polycarpou P, Komodromos P. On the Numerical Simulation of Impacts for the Investigation of Earthquake-Induced Pounding of Buildings, n.d. https://doi.org/10.4203/ccp.93.144.

[10] Ye K, Li L, Zhu H. A note on the Hertz contact model with nonlinear damping for pounding simulation. Earthq Eng Struct Dyn 2009;38:1135–42. https://doi.org/10.1002/eqe.883.

[11] Kun Y. Modified kelvin pounding analytical model. Eng Mech 2009;26:245–8.

[12] Barros RC, Khatami SM. Importance of separation distance on building pounding under near-fault ground motion, using the Iranian earthquake code. 9th Int. Congr. Civ. Eng. Isfahan Univ. Technol. (IUT), Isfahan, Iran, 2012.

[13] Naderpour H, Khatami SM, Barros RC. Creation of a new equation of motion to calculate dissipated energy between two Adjacent Buildings (Compdyn 2015) 2015.

[14] Naderpour H, De Menezes E, Manuel R, Khatami SM. A new model for calculating the impact force and the energy dissipation based on CR-factor and impact velocity. Sci Iran 2015;22:59–68.

[15] Naderpour H, Barros RC, Khatami SM, Jankowski R. Numerical Study on Pounding between Two Adjacent Buildings under Earthquake Excitation. Shock Vib 2016;2016:1–9. https://doi.org/10.1155/2016/1504783.

[16] Naderpour H, Barros RC, Khatami SM. Suggestion of an equation of motion to calculate the damping ratio during earthquake based on a cyclic procedure. J Theor Appl Mech 2016:963. https://doi.org/10.15632/jtam-pl.54.3.963.

[17] Naderpour H, Khatami SM, Barros RC. Prediction of Critical Distance Between Two MDOF Systems Subjected to Seismic Excitation in Terms of Artificial Neural Networks. Period Polytech Civ Eng 2017. https://doi.org/10.3311/PPci.9618.

[18] Muthukumar S, DesRoches R. A Hertz contact model with non-linear damping for pounding simulation. Earthq Eng Struct Dyn 2006;35:811–28. https://doi.org/10.1002/eqe.557.

[19] Goldsmith W. Impact: the Theory and Physical Behavior of Colliding Solids, Edward Arnold Ltd. London, Engl 1960.

[20] Jankowski R, Mahmoud S. Modelling of Structural Pounding, 2015, p. 9–34. https://doi.org/10.1007/978-3-319-16324-6_2.

[21] Jankowski R, Mahmoud S. Earthquake-Induced Structural Pounding. Cham: Springer International Publishing; 2015. https://doi.org/10.1007/978-3-319-16324-6.

[22] Rabiee R, Chae Y. Adaptive base isolation system to achieve structural resiliency under both short- and long-period earthquake ground motions. J Intell Mater Syst Struct 2019;30:16–31. https://doi.org/10.1177/1045389X18806403.

[23] Akbulut M, Sarac A, Ertas AH. An investigation of non-linear optimization methods on composite structures under vibration and buckling loads. Adv Comput Des 2020;5:209–31.

[24] Khatami SM, Naderpour H, Mortezaei A, Maddah M, Lasowicz N, Jankowski R. Optimum shapes and dimensions of rubber bumpers in order to reduce structural pounding during seismic excitations. Structures 2023;48:1046–56. https://doi.org/10.1016/j.istruc.2023.01.026.

[25] Khatami SM, Matos JC, Naderpour H, Mortezaei A, Maddah M. Enhancing Pounding Hazard Assessment: Investigating Rubber Bumper Behavior in Base Isolation Systems during Earthquakes. Pract Period Struct Des Constr 2024;29. https://doi.org/10.1061/PPSCFX.SCENG-1379.

[26] Khatami SM, Naderpour H, Mortezaei A, Sharbatdar A, Lasowicz N, Jankowski R. The Effectiveness of Rubber Bumpers in Reducing the Effects of Earthquake-Induced Pounding between Base-Isolated Buildings. Appl Sci 2022;12:4971. https://doi.org/10.3390/app12104971.

[27] Khatami SM, Naderpour H, Mortezaei AR, Barros RC, Maddah M. The effect of rubber bumper in order to suggest a new equation to calculate damping ratio, subjected building pounding during seismic excitation. Earthquakes Struct 2022;23:129.